

# Investigation of the Photolysis of Phosphites by Time-Resolved Electron Spin Resonance

Igor V. Koptug,<sup>†,‡</sup> Naresh D. Ghatlia,<sup>†,§</sup> Gregory W. Sluggett,<sup>†</sup>  
Nicholas J. Turro,<sup>\*,†</sup> Srinivasan Ganapathy,<sup>†</sup> and Wesley G. Bentrude<sup>\*,†,⊥</sup>

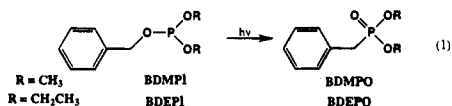
Contribution from the Departments of Chemistry, Columbia University,  
New York, New York 10027, and University of Utah, Salt Lake City, Utah 84112

Received May 8, 1995<sup>⊗</sup>

**Abstract:** The photochemistry of benzyl dimethyl phosphite (BDMPI), *p*-acetylbenzyl dimethyl phosphite (ABDPI) and 1-naphthylmethyl dimethyl phosphite (NMDPI) has been investigated by continuous wave time-resolved electron spin resonance (ESR) and Fourier transform time-resolved ESR techniques. The analysis of the detected ESR signals and their polarization patterns and temporal evolution elucidates the nature of the radical intermediates and the reaction pathway leading to their formation. No ESR signals were detected upon direct photolysis of BDMPI and NMDPI, consistent with a concerted reaction mechanism or predominant formation of a singlet radical pair. In sharp contrast to this, both *p*-acetylbenzyl and dimethoxyphosphonyl radicals have been detected upon direct photolysis of ABDPI in solution. The E\*/A polarization patterns of the two radicals and their temporal evolution are consistent with the triplet reaction pathway. This is further confirmed by the triplet-sensitized photolysis of NMDPI, which yields the dimethoxyphosphonyl radical with the same E\*/A polarization pattern. To make the analysis of spin polarization complete, the zero-field splitting parameters and relative population rates of the triplet sublevels of the molecular triplets of ABDPI and TMDPO ((2,4,6-trimethylbenzoyl)diphenylphosphine oxide) have been determined. These results in combination with product studies show that the direct photolysis of ABDPI proceeds via a triplet precursor to a significant extent.

## Introduction

The photochemical rearrangements of benzylic dimethyl phosphites to benzylphosphonates, a photo-Arbusov reaction, have been shown to occur in good yields and to be applicable to the preparation of benzylphosphonic acid analogs of active antivirals.<sup>1,2</sup> The reaction is regiospecific for the benzyl group and occurs stereospecifically at phosphorus.<sup>3</sup> The configuration of the migrating benzylic carbon is largely *but not totally* retained.<sup>4,5</sup> Obvious mechanisms for this photorearrangement include (i) a predominant concerted, four-electron 1,2-sigmatropic shift, (ii) recombination of short-lived singlet free radical pairs (RP), or (iii) a combination of the above. However, photolysis of benzyl diethyl phosphite (BDEPI, R = CH<sub>2</sub>CH<sub>3</sub>; eq 1) in benzene also generates ~1% yield of bibenzyl,

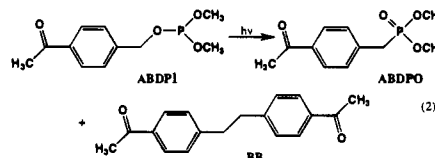


obviously the product of benzyl radical dimerization, suggesting the possible participation of a minor triplet component. It

occurred to us that it should be possible to encourage the formation of triplets by enhancing intersystem crossing in the phosphite or by triplet sensitization of phosphite photochemistry. To test the first hypothesis, the photochemistry of *p*-acetylbenzyl dimethyl phosphite (ABDPI) (eq 2), the *p*-acetyl derivative of benzyl dimethyl phosphite (BDMPI, R = CH<sub>3</sub>; eq 1), was investigated. It was anticipated that ABDPI, because of the well-established rapid intersystem crossing of acetophenone derivatives, should demonstrate significant triplet reactivity, and therefore the formation of free radical products should become significant. To test the second hypothesis, the photochemistry of 1-naphthylmethyl dimethyl phosphite (NMDPI; eq 4), a naphthyl analog of BDMPI, was investigated. It was anticipated that NMDPI, because of the ease of triplet energy transfer to the naphthyl group, could be induced to demonstrate significant triplet reactivity through triplet sensitization.

## Results and Discussion

**Evidence for Participation of Triplets and Free Radicals from Product Analysis.** In striking contrast to the photochemistry of BDEPI, photoexcitation of ABDPI (eq 2) in benzene



yields, at about 10% phosphite conversion, significant amounts of products suggestive of radical cage escape and only a minor amount of rearrangement product, dimethyl (*p*-acetylbenzyl)-phosphonate (ABDPO). Thus, the free radical coupling product *p,p*-diacetylbibenzyl (BB) (eq 2) is formed in 24% yield, whereas the yield of ABDPO is only 12% ( $\Phi_{\text{products}} \approx 0.4$ ; ABDPO, BB). The bulk of the remainder of the products are

<sup>†</sup> Columbia University.

<sup>‡</sup> Permanent address: Institute of Chemical Kinetics and Combustion, Novosibirsk 630090, Russia.

<sup>§</sup> Present address: Unilever Research US, Edgewater, NJ 07020.

<sup>⊥</sup> University of Utah.

<sup>⊗</sup> Abstract published in *Advance ACS Abstracts*, September 1, 1995.

(1) Bentrude, W. G.; Mullah, K. B. *Nucleosides Nucleotides* 1994, 13, 127.

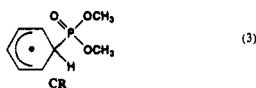
(2) Bentrude, W. G.; Mullah, K. B. *J. Org. Chem.* 1991, 56, 7218.

(3) Cairns, S. M.; Bentrude, W. G. *Tetrahedron Lett.* 1989, 30, 1025.

(4) Omelanzuk, J.; Sopchik, A. E.; Lee, S.-G.; Akutagawa, K.; Cairns, S. M.; Bentrude, W. G. *J. Am. Chem. Soc.* 1988, 110, 6908.

(5) Recent unpublished work of W. Bhanthumnavin, the University of Utah, that employs chiral-column HPLC techniques shows that the 2-phenylethyl dimethyl phosphite (enantiomer ratio ca. 97/3) gives the corresponding phosphonate in an enantiomer ratio of about ca. 85/15.

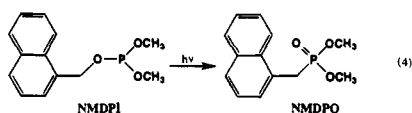
derived from addition of the dimethoxyphosphonyl radical,  $(\text{MeO})_2\text{P}(\text{O})^\bullet$ , to benzene to give the substituted cyclohexadienyl radical (CR; eq 3). The latter is trapped as the 1,2- and 1,4-



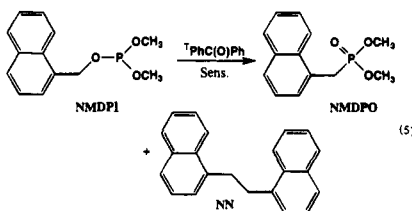
cyclohexadiene products of its reaction with *p*-acetylbenzyl radical, along with lesser amounts of 4'-methylacetophenone and dimethyl phenylphosphonate,  $\text{PhP}(\text{O})(\text{OMe})_2$  (28%).<sup>6</sup>

Photolysis in degassed acetonitrile yields a similar array of products (with the exception of those involving addition to benzene). Addition of thiophenol ( $\text{C}_6\text{H}_5\text{SH}$ ) to the reaction in benzene eliminated the formation of BB in favor of 4'-methylacetophenone and most of the  $\text{PhP}(\text{O})(\text{OMe})_2$  and greatly reduced the yield of ABDPO.<sup>6</sup>

NMDPI, upon direct photoexcitation behaves similarly to BDEPI, efficiently undergoing rearrangement to the corresponding phosphonate, dimethyl (1-naphthylmethyl)phosphonate (NMDPO; eq 4). Photolysis in cyclohexane at 266 nm proceeds



with good efficiency ( $\Phi_{\text{products}} \approx 0.5$ ) and yields 70% of NMDPO and only 0.5% of the free radical coupling product 1,2-di- $\alpha$ -naphthylethane. However, significant amounts of free radical derived products are produced upon triplet photosensitization of NMDPI with benzophenone (eq 5). The yields in



benzene are 12% NMDPO and 16% 1,2-di- $\alpha$ -naphthylethane (NN; eq 5) along with dimethyl phenylphosphonate and 1-methylnaphthalene. Also, the trapping products from phosphonyl radical addition to benzene have been detected. A full account of product studies for ABDPI and NMDPI in various solvents will be published separately.<sup>6</sup>

The results outlined above suggest the significant involvement of triplet RPs in the triplet photosensitized reaction of NMDPI and upon direct photolysis of ABDPI. Below we present evidence for the involvement of triplet excited states in these photoreactions from time-resolved electron spin resonance (TR ESR) investigations of the structure and dynamics of radicals produced by direct photolysis of ABDPI and triplet-sensitized reaction of NMDPI at room temperature, and from the triplet ESR spectrum of ABDPI at 20 K.

**Time-Resolved Electron Spin Resonance Investigation of the Photochemistry of ABDPI and NMDPI.** All our attempts to detect TR ESR signals upon direct laser excitation of BDMPI were unsuccessful. This result is consistent with the rearrangement proceeding primarily via a short-lived singlet RP or concertedly. On the other hand, both continuous wave TR ESR (CW TR ESR) and Fourier transform TR ESR (FT TR ESR) spectra of transient radicals produced upon laser photolysis of ABDPI are readily observed. The CW TR ESR spectrum detected upon photolysis of ABDPI in benzene (Figure 1a)

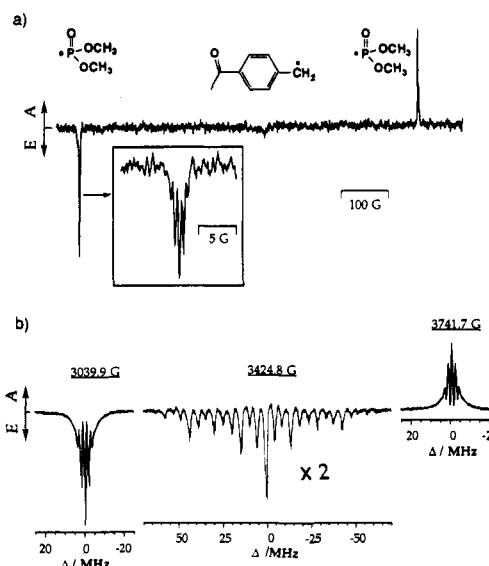


**Figure 1.** TR ESR spectra detected upon direct photolysis of ABDPI in benzene. (a) CW TR ESR spectrum; the boxcar integration gate open in the 150–450 ns time window after the laser flash. The inset shows the low-field component of the phosphonyl doublet detected with the width 1–1.5  $\mu\text{s}$ . (b) FT TR ESR spectra; the 90° mw pulse applied 50 ns after the laser flash. All the signals above the baseline are in absorption (A), and those below the baseline are in emission (E).

clearly shows the presence of the dimethoxyphosphonyl radical with a  $^{31}\text{P}$  hyperfine coupling constant (hfcc) of ca. 700 G, which is similar to the value of 697 G reported in the literature.<sup>7,8</sup> At longer delays, the lines of the dimethoxyphosphonyl radical in the CW TR ESR spectrum develop superhyperfine structure due to a small hfcc with six hydrogen atoms of the two methoxy groups ( $A = 0.60 \pm 0.03$  G), as shown in the inset of Figure 1a. Thus, the formation of the dimethoxyphosphonyl radical in the photolysis of ABDPI is unambiguous. At the same time, the origin of the weak ESR signals in the center of the spectrum (cf. Figure 1a) as well as their polarization pattern is unclear even if the spectra are taken with much narrower field sweep widths.

To identify the paramagnetic species contributing to the center of the ESR spectrum (Figure 1), we employed the FT TR ESR technique because of its inherent ability to perform extensive signal averaging without substantial sample depletion. At the same time, the detection bandwidth in the FT ESR experiment is at least an order of magnitude smaller than the width of the spectrum in Figure 1a, and thus the spectrum must be detected in three separate experiments (Figure 1b). As in the case of the CW TR ESR experiment, both components of the dimethoxyphosphonyl radical doublet show well-resolved hydrogen hyperfine structure, and an E\*/A polarization pattern is apparent. In contrast to the CW TR ESR spectrum, the central portion of the spectrum was detected with the signal-to-noise ratio and spectral resolution sufficient for an unambiguous assignment to the *p*-acetylbenzyl radical. The latter shows net emissive polarization, upon which some E/A polarization is superimposed. The identity of the *p*-acetylbenzyl radical was confirmed by its alternate independent generation through the photolysis of *p*-acetyldeoxybenzoin which produced a spectrum identical to that shown in Figure 1b (except for small differences in the polarization pattern). Thus, our TR ESR results unambiguously show the formation of the dimethoxyphosphonyl and the *p*-acetylbenzyl radicals upon photolysis of ABDPI in solution (cf. eq 6).

(6) Bentrude, W. G.; Ganapathy, S.; Soma Sekhar, B. B. V. To be published.

(7) Davies, A. G.; Griller, D.; Roberts, B. P. *J. Am. Chem. Soc.* **1972**, *94*, 1782.

(8) Roberts, B. P.; Singh, K. *J. Organomet. Chem.* **1978**, *159*, 31.

**Table 1.** Best Fit Parameters Obtained for Molecular Triplets of TMDPO and ABDPI at 20 K

triplet	$D^a/(10^{-1} \text{ cm}^{-1})$	$E^a/(10^{-3} \text{ cm}^{-1})$	$p_X^b$	$p_Y^b$	$p_Z^b$	fwhm <sup>c</sup> /G
TMDPO	$1.868 \pm 0.007$	$7.84 \pm 0.62$	0.1	$0.1 \pm 0.03$	$0.8 \pm 0.25$	$217 \pm 5$
ABDPI	$1.741 \pm 0.013$	$19.4 \pm 1.1$	$0.34 \pm 0.02$	$0.56 \pm 0.03$	0.1	$428 \pm 15$

<sup>a</sup>  $D$  and  $E$  are taken to be positive. <sup>b</sup> The smallest population is taken as 0.1. <sup>c</sup> The Gaussian line shape was used for individual lines.

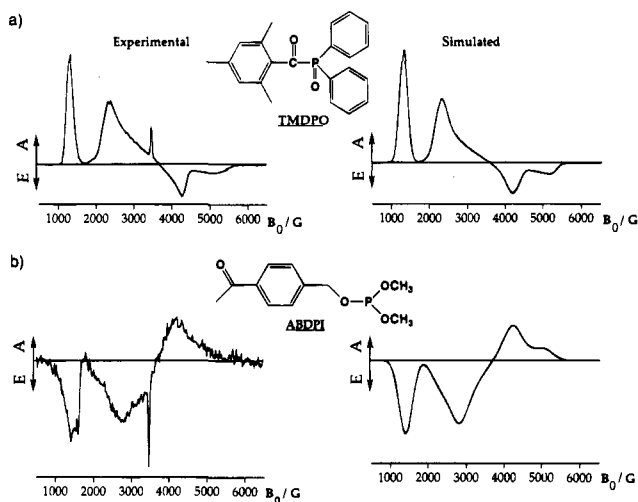
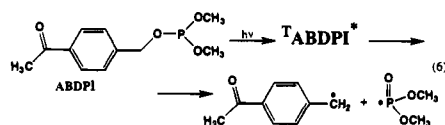


**Figure 2.** Experimental and simulated TR ESR spectra of the randomly oriented molecular triplets of TMDPO and ABDPI. (a) Experimental spectrum of TMDPO in toluene/ethanol glass at 20 K (left) and its simulation (right). (b) Experimental (left) and simulated (right) spectra of ABDPI. Simulation parameters are summarized in Table 1.



CIDEP (chemically induced dynamic electron polarization) effects are known to depend upon the multiplicity of the RP formed upon dissociation of a substrate.<sup>9–11</sup> This important characteristic of CIDEP allows investigation of the involvement of the triplet state of ABDPI upon its photolysis. The mechanisms conventionally considered in producing radical CIDEP in homogeneous solutions<sup>9–14</sup> are (i) the triplet mechanism (TM), (ii) the  $T_0$ -S mechanism, and (iii) the T--S mechanism. Another important mechanism of CIDEP, radical-triplet pair,<sup>15–18</sup> is not considered here, because the triplet lifetime of ABDPI is relatively short.<sup>19</sup>

We begin the mechanistic discussion with the TM, because unlike other mechanisms it contributes only to the initial CIDEP

(9) *Chemically Induced Magnetic Polarization*; Muus, L. T., Atkins, P. W., McLauchlan, K. A., Pedersen, J. B., Eds.; Reidel: Dordrecht, The Netherlands, 1977.

(10) Hore, P. J.; Joslin, C. G.; McLauchlan, K. A. In *Electron Spin Resonance*; Ayscough, P. B., Ed. *Spec. Period. Rep.* **1979**, 5, 1–45.

(11) Salikhov, K. M.; Molin, Y. N.; Sagdeev, R. Z.; Buchachenko, A. L. *Spin Polarization and Magnetic Effects in Radical Reactions*; Elsevier: Amsterdam, 1984.

(12) Hore, P. J.; Joslin, C. G.; McLauchlan, K. A. *Chem. Soc. Rev.* **1979**, 8, 29.

(13) Trifunac, A. D.; Thurnauer, M. C. In *Time Domain Electron Spin Resonance*; Kevan, L., Schwartz, R. N., Eds.; Wiley-Interscience: New York, 1979; pp 107–152.

(14) Depew, M. C.; Wan, J. K. S. *Magn. Reson. Rev.* **1983**, 8, 85.

(15) Blattler, C.; Jent, F.; Paul, H. *Chem. Phys. Lett.* **1990**, 166, 375.

(16) Kawai, A.; Ohi, K. *J. Phys. Chem.* **1992**, 96, 5701.

(17) Goudsmit, G.-H.; Paul, H.; Shushin, A. I. *J. Phys. Chem.* **1993**, 97, 13243.

(18) Turro, N. J.; Koptuyg, I. V.; van Willigen, H.; McLauchlan, K. A. *J. Magn. Reson., Ser. A* **1994**, 109, 121.

(19) Preliminary flash-photolysis experiments in which the formation of the *p*-acetylbenzyl radical monitored at  $\lambda_{\text{max}} = 315 \text{ nm}$  was quenched with various concentrations of 2,5-dimethyl-2,4-hexadiene yield the triplet lifetime for ABDPI on the order of 4 ns.

observed at the earliest time after the laser flash due to the short triplet lifetime and fast spin-lattice equilibration of sublevel populations in the triplet.<sup>11,12,20,21</sup> If operative, the TM would lead to the net polarization of both radicals, scaling their ESR spectra but preserving the binomial ratio of the line intensities.<sup>22</sup> The sign (E or A) of TM polarization is determined by the relative populations of the three triplet sublevels of the precursor substrate molecule at the instant of cleavage. These populations can be investigated by studying the low-temperature TR ESR spectra of molecular triplets in an organic glass.<sup>23</sup>

We have detected (Figure 2) the CW TR ESR spectra of the molecular triplets of ABDPI and TMDPO ((2,4,6-trimethylbenzoyl)diphenylphosphine oxide) in toluene/ethanol glass at 20 K. TMDPO is known to yield strong absorptive polarization of the radicals formed upon photocleavage in solution<sup>24–26</sup> and can be used as a standard for the sign of TM polarization. The experimentally detected spectrum of TMDPO along with its simulation is shown in Figure 2a. The simulation parameters, which are summarized in Table 1, indicate a preferential population of the lowest sublevel of the TMDPO triplet (the three energy levels are chosen to be in the order  $X > Y > Z$ ). The rapid  $\alpha$ -cleavage of the TMDPO triplet with an overpopulated Z sublevel preferentially leads to the overpopulation of the lowest levels of the radicals and thus to their absorptive polarization.<sup>22,27</sup> The experimental and simulated ESR spectra of the triplet ABDPI are shown in Figure 2b. Comparison with Figure 2a shows that the spectrum of ABDPI has an appearance which is an “inverted” form of that for TMDPO, which indicates an “inversion” of the level populations as one goes from TMDPO to ABDPI. Indeed, the simulation parameters in Table 1 indicate the preferential population of the highest sublevels of the ABDPI triplet, which implies overpopulation of the highest energy levels of the radicals formed upon  $\alpha$ -cleavage of triplet ABDPI. It is to be noted that the signal from the ABDPI triplet is substantially weaker than that of TMDPO under the same experimental conditions. In any case, we conclude from these results that the polarization of both radicals formed upon cleavage of triplet ABDPI in solution, if observable, is expected to be emissive.

The two other polarization mechanisms,  $T_0$ -S and T--S, both contribute to the temporal evolution as well as initial polarization of the ESR spectra. The “pure”  $T_0$ -S polarization mechanism yields a symmetric E/A pattern (low-field half of a spectrum in emission, high-field half in absorption) in the case of a triplet RP and an A/E pattern in the case of a singlet RP for both participating radicals. The net contribution from the  $T_0$ -S mechanism is expected to be small in the systems investigated here since the difference in the  $g$  factors of the

(20) Bowman, M. K. In *Modern Pulsed and Continuous-Wave Electron Spin Resonance*; Kevan, L., Bowman, M. K., Eds.; Wiley-Interscience: New York, 1990; pp 1–42.

(21) Ohara, K.; Murai, H.; Kuwata, K. *Bull. Chem. Soc. Jpn.* **1992**, 65, 1672.

(22) McLauchlan, K. A. In *Modern Pulsed and Continuous-Wave Electron Spin Resonance*; Kevan, L., Bowman, M. K., Eds.; Wiley-Interscience: New York, 1990; pp 285–363.

(23) Hirota, N.; Yamauchi, S. In *Dynamics of Excited Molecules*; Kuchitsu, K., Ed.; Elsevier: Amsterdam, 1994; Vol. 82; pp 513–557.

(24) Baxter, J. E.; Davldson, R. S.; Hageman, H. J.; McLauchlan, K. A.; Stevens, D. G. *J. Chem. Soc., Chem. Commun.* **1987**, 73.

(25) Kamachi, M.; Kuwata, K.; Sumiyoshi, T.; Schnabel, W. *J. Chem. Soc., Perkin Trans. 2* **1988**, 961.

(26) Turro, N. J.; Khudyakov, I. V. *Chem. Phys. Lett.* **1992**, 193, 546.

(27) Atkins, P. W.; Evans, G. T. *Mol. Phys.* **1974**, 27, 1633.

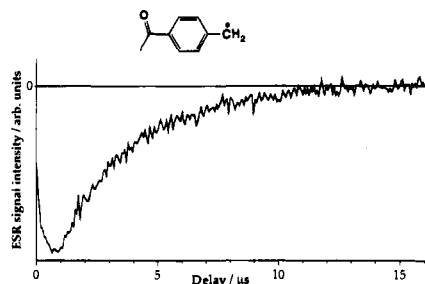


**Figure 3.** Temporal evolution of the *p*-acetylbenzyl radical polarization detected by the FT TR ESR technique upon direct photolysis of ABDPI.

two radicals is negligible as compared to the phosphorus hfcc ( $g(\text{dimethoxyphosphonyl}) = 2.0018$ ,<sup>8</sup>  $g(p\text{-acetylbenzyl}) = 2.0029$ ,<sup>50</sup>  $\Delta gB_0 \approx 3.8 \text{ G} \ll A = 700 \text{ G}$ ). The T<sub>0</sub>-S mechanism is relatively rare because it can only be operative under specific conditions, such as high viscosity or low temperature, which restrict the relative diffusion of the radicals.<sup>28-32</sup> However, it has been shown that T<sub>0</sub>-S CIDEP can be observed in nonviscous solutions at room temperature for radicals possessing an exceptionally large hfcc,<sup>33</sup> such as P-centered radicals.<sup>34-36</sup> CIDEP in this mechanism is created in the transition T<sub>0</sub>- $\alpha \rightarrow S\beta$ , ( $\alpha, \beta$ -nuclear spin states) which involves a simultaneous flip of one of the electron spins and a nuclear spin in the triplet RP. If this mechanism is operative in our case, it is solely due to the large hfcc with the <sup>31</sup>P nucleus, and it is the latter nuclear spin (and not those of hydrogen atoms) which flips in the T<sub>0</sub>- $\alpha \rightarrow S\beta$  transition. This should lead to the hyperfine-dependent polarization for the dimethoxyphosphonyl radical. The T<sub>0</sub>-S mechanism is thus expected to contribute emission to the low-field line which corresponds to the  $\alpha$  nuclear spin state, and no polarization to the high-field line. On the other hand, for the *p*-acetylbenzyl radical the intensity ratio of the ESR lines is expected to be close to binomial in the T<sub>0</sub>-S mechanism.<sup>22,35</sup>

To discuss the contributions of these two mechanisms to CIDEP and to determine the multiplicity of the precursor, it is essential to examine the temporal evolution of CIDEP for both radicals. The FT TR ESR technique is especially suitable for measuring CIDEP kinetics.<sup>37</sup> Its advantage over the CW TR ESR technique is the absence of the microwave (mw) field during the detection period, for the latter is known to complicate the analysis of CW TR ESR kinetic data.<sup>20,38</sup> Figure 3 shows the temporal evolution of the *p*-acetylbenzyl radical polarization following pulsed laser photolysis of ABDPI. Detection of the entire spectra at different delays shows that the observed pattern remains unchanged; i.e., the spectrum of *p*-acetylbenzyl radical evolves as a single entity. Two important features of the observed trace are the initial emissive polarization at zero time and a continuing formation of emissive polarization up to about 1  $\mu\text{s}$  after the laser flash. For the dimethoxyphosphonyl radical, the initial emissive polarization is observed for the low-field line (Figure 4a, curve 1) and absorptive polarization for the high-

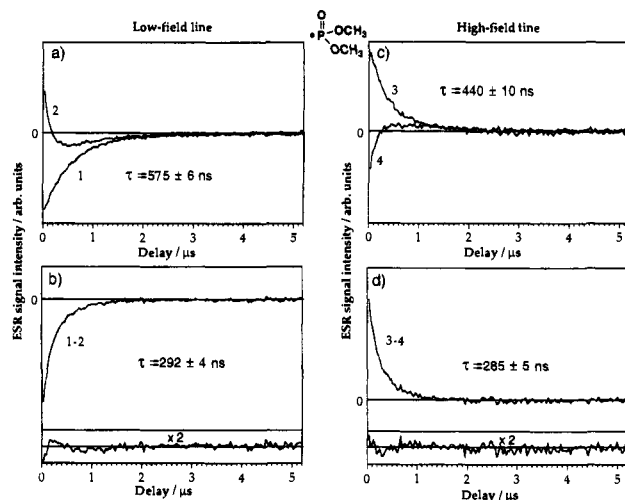


**Figure 4.** Temporal evolution of the two components of the phosphonyl doublet. (a) Unperturbed evolution of the low-field component (trace 1) and evolution after a perturbation with a 180° pulse immediately after the laser flash (trace 2). (c) The same for the high-field component: trace 3, unperturbed evolution; trace 4, after perturbation with a 180° pulse. (b, d) Differences between the unperturbed and perturbed traces and the residuals of the exponential fit for the low-field and high-field components of the phosphonyl doublet, respectively.

field line (Figure 4c, curve 3), with the absolute intensity of the low-field line being somewhat larger (cf. Figure 1b). The two traces are close to single-exponential decays with substantially different characteristic decay times of  $\tau = 575 \pm 6 \text{ ns}$  for the low-field line and  $\tau = 440 \pm 10 \text{ ns}$  for the high-field one.

The initial E/A polarization of the dimethoxyphosphonyl radical and a small E/A contribution to the spectrum of the *p*-acetylbenzyl radical clearly point to the T<sub>0</sub>-S spin evolution in the triplet geminate RP and thus to the triplet state of ABDPI producing these radicals. The predominance of the emissive polarization for *both* radicals immediately after the flash can be due to either the TM or the T<sub>0</sub>-S evolution in the triplet geminate pair. Thus, all of the possible mechanisms imply that the triplet reaction channel operates in the photolysis of ABDPI (eq 6).

The CIDEP kinetics of the dimethoxyphosphonyl radical (Figure 4) clearly demonstrates that polarization buildup continues for the radicals which survived the geminate stage and escaped into the bulk. The slower apparent decay of the *low-field* component of the phosphonyl doublet is caused by the competition of the polarization decay and its continuing formation due to the T<sub>0</sub>-S mechanism, and is not due to the differences in their spin-lattice relaxation times. This can be verified by the dynamic polarization recovery technique.<sup>39</sup> In this experiment an ESR signal is perturbed with a mw pulse immediately after the laser flash, and the subsequent temporal evolution of the perturbed magnetization is monitored. Due to the large phosphorus hfcc this can be done selectively for each component of the phosphonyl doublet without any interference from the other ESR signals. A nominal 180° pulse was employed as a perturbation, and the subsequent temporal evolutions of the low-field and high-field phosphonyl lines are depicted in parts a (curve 2) and c (curve 4), respectively, of Figure 4. Especially from Figure 4a it is clear that a substantial polarization is created in the free encounters of radicals which is sufficient to invert back the perturbed line. More importantly, the time-dependent rate of polarization formation is expected to be the same for the perturbed and unperturbed recovery curves. Thus, taking a difference cancels its contribution and

(28) Trifunac, A. D.; Nelson, D. J. *Chem. Phys. Lett.* **1977**, *46*, 346.

(29) Honma, H.; Murai, H.; Kuwata, K. *Chem. Phys. Lett.* **1992**, *195*, 239.

(30) Trifunac, A. D. *Chem. Phys. Lett.* **1977**, *49*, 457.

(31) Koptuyg, I. V.; Lukzen, N. N.; Bagryanskaya, E. G.; Doktorov, A. B.; Sagdeev, R. Z. *Chem. Phys.* **1992**, *162*, 165.

(32) Closs, G. L.; Forbes, M. D. E.; Plotrowiak, P. *J. Am. Chem. Soc.* **1992**, *114*, 3285.

(33) Trifunac, A. D.; Nelson, D. J. *J. Am. Chem. Soc.* **1977**, *99*, 289.

(34) Adrian, F. J.; Akiyama, K.; Ingold, K. U.; Wan, J. K. S. *Chem. Phys. Lett.* **1989**, *155*, 333.

(35) Buckley, C. D.; McLauchlan, K. A. *Chem. Phys. Lett.* **1987**, *137*, 86.

(36) Burkey, T. J.; Luszyk, J.; Ingold, K. U.; Wan, J. K. S.; Adrian, F. J. *J. Phys. Chem.* **1985**, *89*, 4286.

(37) van Willigen, H.; Levstein, P. R.; Ebersole, M. H. *Chem. Rev.* **1993**, *93*, 173.

(38) Hore, P. J.; McLauchlan, K. A. *Mol. Phys.* **1981**, *42*, 533.

(39) Bartels, D. M.; Lawler, R. G.; Trifunac, A. D. *J. Chem. Phys.* **1985**, *83*, 2686.

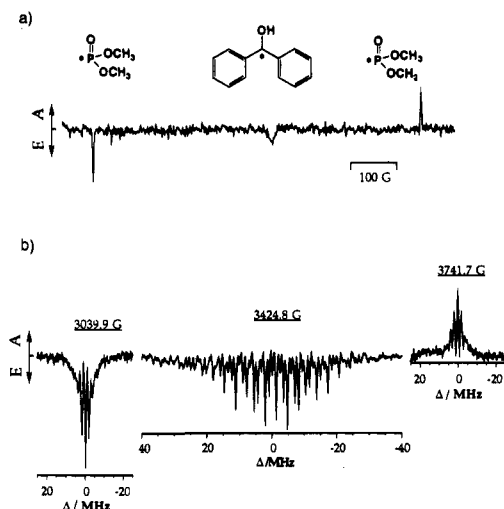


**Figure 5.** TR ESR spectra detected upon benzophenone-sensitized photolysis of NMDPI in benzene. (a) CW TR ESR spectrum; the boxcar integration gate open in the 0.25–1  $\mu$ s time window after the laser flash. (b) FT TR ESR spectra; the 90° mw pulse applied 0.5  $\mu$ s (dimethoxyphosphonyl radical) or 4.5  $\mu$ s (benzophenone ketyl radical) after the laser flash.

leaves only the magnetization decay due to spin–lattice relaxation, chemical decay, etc. The two resulting difference curves 1–2 (Figure 4b) and 3–4 (Figure 4d) yield good single-exponential fits with almost identical decay times  $\tau = 292 \pm 4$  ns and  $\tau = 285 \pm 5$  ns. This gives a lower-limit estimate of the spin–lattice relaxation time of the dimethoxyphosphonyl radical as  $T_1 \geq 300$  ns. However, it is likely that the true value of  $T_1$  is somewhat larger since other magnetization decay mechanisms (e.g., chemical decay, spin exchange) contribute to the difference traces.

As in the case of BDMPI, we failed to detect any TR ESR signals upon direct 308 nm pulsed excitation of the naphthyl analog, NMDPI. Upon triplet sensitization, however, the dimethoxyphosphonyl radical doublet is clearly observed in both CW TR ESR and FT TR ESR spectra. For example, the CW TR ESR spectrum detected upon triplet sensitization of NMDPI with benzophenone is shown in Figure 5a. The phosphonyl radical shows the same E\*/A polarization pattern (although substantially weaker) as in the case of the direct photolysis of ABDPI, consistent with the triplet multiplicity of the RP precursor in both cases. The ESR signal in the center of the spectrum, however, is that of the benzophenone ketyl radical,<sup>40</sup> and not that of the 1-naphthylmethyl radical. This is clearly seen in the well-resolved FT TR ESR spectra shown in Figure 5b. Similar spectra were detected with xanthone as the triplet sensitizer, in which case both phosphonyl and xanthone ketyl radicals were clearly observed.

The mechanism responsible for the formation of the sensitizer ketyl radicals is not clear at present. It appears, however, that they acquire substantial emissive polarization in the presence of the dimethoxyphosphonyl radicals as a result of T<sub>1</sub>–S evolution in F-pairs, similar to the *p*-acetylbenzyl radical in the direct photolysis of ABDPI. To exclude this side reaction, we used 4'-methoxyacetophenone and triphenylene as triplet sensitizers. In both cases the formation of the dimethoxyphosphonyl radical (E\*/A pattern) is readily detected. The contribution of the 1-naphthylmethyl radical, however, is too weak to be detected with a S/N ratio sufficient for its unambiguous identification. Interestingly, the reported ESR spectra of naphthylmethyl radicals show poor resolution and/or sensitivity.<sup>41,42</sup> As a control, we photolyzed NMDPI in the presence

of benzil. No signals of the dimethoxyphosphonyl radical were detected as expected, since the triplet energy of benzil ( $E_T = 53.4$  kcal/mol)<sup>43</sup> is lower than that of NMDPI (for 1-methylnaphthalene  $E_T = 59.6$  kcal/mol).<sup>43</sup>

## Conclusions

In this work we have shown that the reaction pathway of a photo-Arbuzov rearrangement of benzylic phosphites can be altered by introducing a moiety which enhances intersystem crossing in a photoexcited phosphite or through triplet sensitization. While BDMPI, BDEPI, and NMDPI undergo rearrangement primarily via a singlet radical pair or concertedly, introduction of a *p*-acetyl group in ABDPI forces the reaction into the triplet reaction pathway, as evidenced by the TR ESR detection of *p*-acetylbenzyl and dimethoxyphosphonyl radicals and the analysis of their spin polarization. Observation of a similarly polarized spectrum of the dimethoxyphosphonyl radical after a direct formation of a triplet phosphite upon triplet-sensitized photolysis of NMDPI lends further support for the significant involvement of triplets in this photolysis. A quantitative analysis of a triplet *vs* singlet reaction pathway is not possible, however, as the ESR signal intensities are determined by several mechanisms of CIDEP. Further work is in progress, including chemically induced dynamic nuclear polarization (CIDNP) and product studies.

## Experimental Section

**Chemicals and Instrumentation.** Prior to use in photochemical experiments, benzene (Baker Photrex reagent) was distilled from sodium and omnisolve spectrograde acetonitrile (EM Science) was distilled from calcium hydride.

For TR ESR experiments the solvents in their purest commercially available form were used as received. TMDPO was obtained from BASF (Germany) and recrystallized from diethyl ether. Benzophenone, 4'-methoxyacetophenone, and xanthone were purchased from Aldrich and recrystallized from ethanol. Preparation of BDMPI, BDEPI, ABDPI, and NMDPI and their photolysis products will be described elsewhere.<sup>6</sup> The phosphites were purified by molecular distillation in vacuo and sealed under argon.

In the CW TR ESR experiments a direct detection of ESR signals without magnetic field modulation was employed. The solutions were purged with argon and photolyzed with either 308 nm light (XeCl) of a Lambda Physik EMG 100 excimer laser or 266 nm light (the fourth harmonic) of a Quanta Ray DCR 2A Nd:YAG laser in a quartz flow cell (1 mm thick) positioned in the rectangular cavity of an X-band ESR spectrometer (Bruker, ER 100D). The output of the mw bridge broad-band preamplifier (6.5 MHz) was fed into the boxcar averager and signal processor (PAR, models 4420 and 4402). An implementation of a faster photodiode for triggering the boxcar allowed us to reduce the deadtime of the setup from 200 ns<sup>44</sup> down to *ca.* 50 ns, which is taken into account in the integration windows indicated in the figure captions. Further details can be found elsewhere.<sup>45,46</sup>

The direct detection technique was also used for the low-temperature ESR studies of molecular triplets. The same boxcar averager was used in combination with the Bruker ESP-300 X-band ESR spectrometer equipped with a dielectric ring cavity (ESP380-1052 DLQ-H) in a high-Q mode and an Oxford cryostat (GFS 300). Both the cavity and the cryostat are designed to allow optical excitation of the samples which was achieved with the 308 nm light of a Lambda Physik LPX 100 excimer laser. The signals were averaged over a 5  $\mu$ s period following the laser flash. No sample depletion was observed in successive repetitions of the experiments. Solutions of ABDPI or TMDPO in toluene/ethanol mixtures (1:1 by volume) were transferred

(41) Kawai, A.; Okutsu, T.; Obi, K. *Chem. Phys. Lett.* **1990**, *174*, 213.

(42) Jackson, R. A.; Rhodes, C. J. *J. Chem. Soc., Perkin Trans. 2* **1993**, 53.

(43) Murov, S. L.; Carmichael, I.; Hug, G. L. *Handbook of Photochemistry*, 2nd ed.; Marcel Dekker: New York, 1993; pp 1–53.

(44) Koptuyug, I. V.; Ghatia, N. D.; Turro, N. J.; Jenks, W. S. *J. Phys. Chem.* **1993**, *97*, 7247.

(45) Jenks, W. S. Ph.D. Thesis, Columbia University, New York, 1991.

(46) Lipson, M.; McGarry, P. F.; Koptuyug, I. V.; Staab, H. A.; Turro, N. J.; Doetschman, D. C. *J. Phys. Chem.* **1994**, *98*, 7504.

(40) Landolt-Börnstein, *Numerical Data and Functional Relationships in Science and Technology. New Series, group II*; Hellwege, K. H., Fischer, H., Eds.; Springer-Verlag: 1977; Vol. 9b.

to 4 mm o.d. quartz ESR tubes and cooled to 20 K inside the ESR cavity immersed into the cryostat by a permanent flow of evaporating helium. Further details have been reported elsewhere.<sup>46</sup>

FT TR ESR data were collected employing a Bruker ESP-300/380 pulsed ESR spectrometer equipped with a 1 kW TWT amplifier and the overcoupled dielectric ring cavity (90° pulse length 16 ns). A LeCroy 9450A oscilloscope employed as a fast digitizer (400 megasamples/s) allowed the detection of an entire free induction decay (FID) after application of a single mw pulse and a single laser flash. This allows an extensive signal averaging to be performed without substantial sample depletion. For kinetic measurements the sampling digitizer of the ESP-300/380 spectrometer was employed to detect a representative single point of an FID using it as a measure of the signal intensity.<sup>18</sup> By comparison with the detection of the entire spectra at different delays, it has been demonstrated that detection of a single FID point does not introduce any artifacts in the observed kinetics. The samples were prepared in 4 mm o.d. quartz ESR tubes and purged with argon prior to use.

**Quantum Yields.** From Baker Photrex benzene, freshly distilled from sodium, was prepared a solution of ABDPI (0.02 M) and tri-*n*-butyl phosphate as internal standard (50 mM). This solution (3.4 mL) was placed in a 1 cm quartz cuvette and argon saturated for 15 min. The stirred solution was irradiated at 335 nm in a Photon Technology International Quanticount electronic actinometer (precalibrated with potassium ferrioxalate) and sampled at 1561 and 2000 s for GLC analysis on a DB-1 column (flame ionization detector). Conversions of BDEPI were 5–10%. The quantum yields for ABDPO (0.074 ± 0.001), BB (0.142 ± 0.001), and dimethyl phenylphosphonate (0.176 ± 0.002) were thereby determined using predetermined response factors. The above products were identified by GC/MS by comparison with authentic samples.

A similar procedure was used for NMDPI. A 0.025 M solution in hexane was irradiated at 266 nm to 3% and 7% conversions. The quantum yields of NMDPO and 1,2-di- $\alpha$ -naphthylethane are 0.47 and 0.004, respectively.

**Product Yields.** Benzene solutions of ABDPI (0.012 M) containing 0.0, 0.002, 0.013, 0.052, and 0.17 M thiophenol (PhSH) were irradiated with light from a 450 W medium-pressure mercury lamp, filtered through uranium glass to remove light below 340 nm, to 10–16% consumption of ABDPI. The BB yield was reduced to near zero even at 0.002 M concentration of PhSH and to zero at higher concentrations. Simultaneously, major amounts of 4'-methylacetophenone were formed, while the ABDPO yield was reduced to about 3%.

Upon direct photolysis of NMDPI in hexane at 266 nm, the NMDPO yield is 70% and that of 1,2-di- $\alpha$ -naphthylethane is 0.25% at 3–7% consumption of NMDPI. In the case of benzophenone-sensitized photolysis of NMDPI in benzene the yields at 5% conversion are 12% NMDPO and 16% 1,2-di- $\alpha$ -naphthylethane along with dimethyl phenylphosphonate and 1-methylnaphthalene.

Chemical and quantum yields of dimers BB and 1,2-di- $\alpha$ -naphthylethane are based on moles of dimers formed and thus are not corrected for stoichiometry.

**ESR Spectra of Radicals.** The <sup>31</sup>P hfcc of the dimethoxyphosphonyl radical in benzene was found to be  $A = 694.5 \pm 1$  G. We note that it is different from the apparent splitting observed in the experimental spectrum (701.8 G, cf. Figure 1b) and was evaluated by taking into account the second-order corrections<sup>47</sup> to the spin Hamiltonian using 2,2-diphenyl-1-picrylhydrazyl free radical (DPPH;  $g = 2.0036$ ) as a reference. Similarly,  $A = 701.2 \pm 1$  G for the dimethoxyphosphonyl radical in acetonitrile. The difference in the two values is presumably due to the difference in the dielectric constants of the solvents used. The second-order shifts of the doublet components also lead to a low-field shift of the center of gravity of the phosphonyl doublet. This led to an incorrect evaluation of its  $g$ -factor<sup>7</sup> and misinterpretation of some high-field CIDNP data.<sup>48,49</sup> The corrected value of  $g = 2.0018$  was reported later.<sup>8</sup>

The evaluated hfcc values of the *p*-acetylbenzyl radical are very close to those reported<sup>50–53</sup> except for the hfcc of the CH<sub>3</sub> group, which in

fact was not resolved<sup>51–53</sup> but rather estimated from the observed linewidth (0.5 G).<sup>54</sup> Our simulations yield  $A(\text{CH}_3) = 0.21 \pm 0.02$  G (fwhm = 0.08 G, cf. Figure 1b). To verify the assignment of the observed spectrum to the *p*-acetylbenzyl radical, the photolysis of 4-acetyldeoxybenzoin was studied by FT TR ESR in a separate experiment. Upon photoexcitation the ketone cleaves to form *p*-acetylbenzyl and benzoyl radicals. The  $T_2$  relaxation time of the latter is shorter than the detector dead time, and it does not usually show up in FT ESR spectra. Thus, only the ESR spectrum of the *p*-acetylbenzyl radical is observed. Except for a small difference in the polarization patterns, the spectrum detected is identical to that obtained upon photolysis of ABDPI.

**ESR of Molecular Triplets at Low Temperature.** The simulations of the experimental ESR spectra of molecular triplets in a glass are based on the theory of the ESR of randomly oriented triplet molecules developed in the literature.<sup>55–58</sup> The Levenberg–Marquardt least-squares algorithm was implemented to extract the zero-field splitting (ZFS) parameters  $D$  and  $E$  and the relative populations of the three sublevels  $p_X$ ,  $p_Y$ , and  $p_Z$ . Other adjustable parameters are the intrinsic line width of the individual lines (Gaussian line shape) and an isotropic  $g$  factor. The very large line width required in the simulations of the ABDPI spectrum (428 G as compared to 217 G for TMDPO, cf. Table 1) is presumably due to an existence of slightly different molecular conformations in a glass, which leads to a variation of ZFS parameters due to a different mixing of the energetically close <sup>3</sup> $\pi\pi^*$  and <sup>3</sup> $\pi\pi^*$  states, as observed in other aromatic carbonyl compounds.<sup>46</sup> A sharp signal observed in the experimental spectra at  $g = 2$  has been found to decay much slower than the main spectrum. It has been tentatively assigned to a doublet radical and excluded from spectral simulations.<sup>46,55,59</sup>

The sign of polarization of the radicals formed upon reaction of a triplet in solution is given by eq 7, with  $\Gamma > 0$  corresponding to net

$$\Gamma = -\{D(p_X + p_Y - 2p_Z) + 3E(p_X - p_Y)\} \quad (7)$$

absorption and  $\Gamma < 0$  corresponding to net emission.<sup>11,27,60,61</sup> We define  $D$  and  $E$  as  $D = -1.5Z$  and  $E = 0.5(X - Y)$  where  $X = E_{XX}$ ,  $Y = E_{YY}$ , and  $Z = E_{ZZ}$  are the principal values of a traceless spin–spin coupling tensor. Note that in the literature  $E$  is sometimes defined with an opposite sign,<sup>11,27</sup> which changes the sign of the second term in eq 7. The parameters obtained from the simulations are not unique.<sup>47,56,62,63</sup> This however has no effect on the sign of polarization  $\Gamma$ . We adopt the convention which requires that  $|D| \geq 3|E|$ , and choose  $D, E > 0$ . The smallest population is taken as 0.1.

**Acknowledgment.** Support of this work by grants from the National Science Foundation, the National Cancer Institute of the Public Health Service (CA11045) (to W.G.B.), and the Kanagawa Academy of Science and Technology (KAST) (to N.J.T.) is gratefully acknowledged. W.G.B. thanks Professor Cheves Walling for suggesting the use of ABDPI to produce triplet photochemistry. We also thank Ms. Margaret S. Landis and Dr. Xuegong Lei, Columbia University, for the synthesis of 1-naphthylmethyl dimethyl phosphite and 4-acetyldeoxybenzoin, respectively. G.W.S. thanks the Natural Sciences and Engineering Research Council (Canada) for a postdoctoral fellowship.

JA951484F

(51) Dust, J. M.; Arnold, D. R. *J. Am. Chem. Soc.* **1983**, *105*, 1221.

(52) Dust, J. M.; Arnold, D. R. *J. Am. Chem. Soc.* **1983**, *105*, 6531.

(53) Arnold, D. R.; Nicholas, A. M. d. P.; Snow, M. S. *Can. J. Chem.* **1985**, *63*, 1150.

(54) Arnold, D. R. Private communication.

(55) Yager, W. A.; Wasserman, E.; Cramer, R. M. R. *J. Chem. Phys.* **1962**, *37*, 1148.

(56) Kottis, P.; Lefebvre, R. *J. Chem. Phys.* **1963**, *39*, 393.

(57) Kottis, P.; Lefebvre, R. *J. Chem. Phys.* **1964**, *41*, 379.

(58) Wasserman, E.; Snyder, L. C.; Yager, W. A. *J. Chem. Phys.* **1964**, *41*, 1763.

(59) Murai, H.; Imamura, T.; Obi, K. *Chem. Phys. Lett.* **1982**, *87*, 295.

(60) Wong, S. K.; Hutchinson, D. A.; Wan, J. K. S. *J. Chem. Phys.* **1973**, *58*, 985.

(61) Pedersen, J. B.; Freed, J. H. *J. Chem. Phys.* **1975**, *62*, 1706.

(62) Tominaga, K.; Yamauchi, S.; Hirota, N. *J. Phys. Chem.* **1990**, *94*, 4425.

(63) McGlynn, S. P.; Azumi, T.; Kinoshita, M. *Molecular Spectroscopy of the Triplet State*; Prentice-Hall: Englewood Cliffs, NJ, 1969.

(47) Carrington, A.; McLachlan, A. D. *Introduction to Magnetic Resonance*; Harper & Row: New York, 1967.

(48) Levin, Y. A.; Il'yasov, A. V.; Goldfarb, E. I.; Vorkunova, E. I. *Org. Magn. Reson.* **1973**, *5*, 487.

(49) Levin, Y. A.; Il'yasov, A. V.; Goldfarb, E. I.; Vorkunova, E. I. *Org. Magn. Reson.* **1973**, *5*, 497.

(50) Neta, P.; Schuler, R. H. *J. Phys. Chem.* **1973**, *77*, 1368.